TWO-DIMENSIONAL (2D) NANOSILICATES FOR ADDITIVE MANUFACTURING: INK, SUPPORT-BATH AND SACRIFICIAL INK

A Thesis

by

SATYAM RAJPUT

Submitted to the Office of Graduate and Professional Studies of
Texas A&M University
in partial fulfillment of the requirements for the degree of

MASTER OF SCIENCE

Chair of Committee,	Akhilesh K. Gaharwar
Committee Members,	Daniel Alge
	Limei Tian
Head of Department,	Michael McShane

May 2020

Major Subject: Biomedical Engineering

ABSTRACT

The growing need for tissue and organ replacements has resulted in significant increase in the gap between the organ donors and patients on the waitlist. Extrusion based 3D bioprinting technique is a promising approach to bridge the gap by designing patient-specific tissue engineered grafts. However, there is a dearth of materials that can be used for multiple applications related to extrusion-based 3D printing for tissue engineering. In this study, we introduce colloidal solution of two-dimensional (2D) nanosilicates as a platform technology to print complex structure via three different approaches. In first approach, we can design shear-thinning ink by combining nanosilicates in water. This can be extended to polymers that are soluble in water by adding nanosilicates to them. In second approach, we will employ colloidal nanosilicate gel as a support bath for 3D printing that nullifies the surface tension and gravitational forces. In the third approach, we demonstrate use of nanosilicate bioink as a sacrificial ink to design microfluidic devices for printing vascular channel or in vitro disease modelling. The results indicate that these nanosilicates can be successfully used for all the three approaches. Hence, this study establishes the use of nanosilicates as an ink additive, support bath and sacrificial ink for soft matter 3D printing applications. The versatility of nanosilicate-based biomaterials is expected to provide a wide-spread adoption of this technology in the additive manufacturing of soft materials.

DEDICATION

This thesis is dedicated to my father, Mr. S.K. Rajput, my mother, Mrs. Sangita Rajput, and my brother, Mr. Shilpam Rajput. They have been a major source of inspiration to me and have been a pillar of strength throughout my life.

I would also like to dedicate this thesis to all the teachers and mentors that were a part of my life and inspired me to follow my dreams.

ACKNOWLEDGEMENTS

I would like to thank my committee chair, Dr. Akhilesh Gaharwar, for his constant support and guidance and my committee members, Dr. Daniel Alge and Dr. Limei Tian, for their guidance throughout the course of this research. I would also like to thank Dr. Ronald Kaunas, Director of Graduate Programs and Dr. Mike McShane, Head of Biomedical Engineering Department at Texas A&M University for their help and support.

I would also like to thank my lab mates in the Gaharwar lab who have been a big support to me both mentally and emotionally during my master's at A&M. A big thanks to my friends and colleagues and the department faculty and staff for making my time at Texas A&M University a great experience.

CONTRIBUTORS AND FUNDING SOURCES

Contributors

This work was supervised by a thesis committee consisting of Professors Dr. Akhilesh Gaharwar, Dr. Daniel Alge and Dr. Limei Tian of the Department of Biomedical Engineering at Texas A&M University.

All the research work and data contained in the thesis was done by the student. I would like to thank all the members of the Gaharwar lab for their help, useful discussions and suggestions.

Funding Sources

This work was made possible in part by financial support from the National Institute of Biomedical Imaging and Bioengineering (NIBIB) of the National Institutes of Health (NIH) Director's New Innovator Award (DP2 EB026265) and the National Science Foundation (NSF) Award (CBET 1705852). The content is solely the responsibility of the author and does not necessarily represent the official views of the funding agency.

NOMENCLATURE

cGMP	Current Good Manufacturing Practices
CFD	Computational fluid dynamics
GelMA	Gelatin methacryloyl
KCa	Kappa Carrageenan
PDMS	Polydimethylsiloxane
ESC	Embryonic stem cells
MSC	Mesenchymal stem cells
HSC	Hematopoietic stem cells
IPSC	Induced Pluripotent stem cells
VEGF	Vascular endothelial growth cells
ECM	Extra cellular matrix
NGF	Nerve growth factors
HUVECs	Human umbilical vein endothelial cells
SEM	Scanning electron microscopy

TABLE OF CONTENTS

Page

LIST OF FIGURES

Page

CHAPTER I

INTRODUCTION

1.1 Need and Clinical Significance

There is an acute shortage of organs for people in the need of organ replacement in the world. According to the United Network of Organ Sharing (UNOS), there are around 113,000 people on the waitlist for organ donation (as of January 2020)[1]. Although the data suggests a small drop between the supply and demand of organ replacements over the recent years, the number of people waiting for organ transplants is still a very large portion. In 2017, approximately 18 people died every day and more than 6500 died in total while waiting for organ replacement[1]. Moreover, this data only includes patients waiting for transplants in the United States of America. The need for organ donations in the whole world is expected to be significantly higher than the numbers mentioned above.

Categorically, by organ type, kidneys topped the list of organ transplants (21,167) followed by liver (8,250), heart (3,408) and lung (2,530) in 2018 (as of January 2019). Other types of organ transplants include kidney/pancreas (836), pancreas (192), intestine (104), heart/lung (32), vascular allograft (11)[1]. Patients waiting for organ replacement by organ type are loosely in similar proportion. Moreover, successful transplantation of organs is itself a challenging task. First, all transplant candidates on the waiting list that are compatible with the donor are screened and separated based on blood type, height, weight and other medical factors. Then, the computer system determines the order in

which candidates will receive offers. Next, the matching system considers the distance between donor and transplant hospitals. The local candidates get organ offers before those listed at more distant hospitals. The allocation, transport and transplantation of the organ takes quite some time and that requires preserving the organ for a certain amount of time. The maximum time that different types of organs can be preserved for are: kidneys (24-36 hours), pancreas (12-18 hours), liver (8-12 hours) and heart or lung (4-6 hours)[2]. Hence, the time frame for preserving these organs is very short. Additionally, one major important consideration for successful transplant is the use of right sized organ. Usually, children respond better to child sized organs. These numbers only represent transplantation of functional organs.

If other tissues/organs such as skin, bone, cartilage, cornea, vessels, etc are included then the total number of cases going under some form of interventional procedure becomes significantly more. Two seminal papers on tissue engineering[3, 4] by Robert Langer and Joseph Vacanti from 1990's provide an overview of the number of cases going through surgical procedures for different types of tissue and organ diseases and impairment. As more American population reaches old age and lives longer compared to previous generations, these cases are expected to rise exponentially. Again, these statistics are just for the American population and if the world population is considered, the numbers would be far greater. Especially, in developing continents such as Asia and Africa where the healthcare innovations and technologies reach much later compared to developed countries, the prevalence of such cases is expected to be higher as a below par quality treatment is expected. Apart from this, the pharmaceutical industry is facing decline in the

the R&D productivity, ie, it is becoming more and more difficult for clinical translation of new drugs. One of the main reasons is the use of animals for clinical testing which don't exactly mimic the human physiology.

According to the US Department of Health and Human Service report titled "2020: A New Vision-A Future for Regenerative Medicine", the annual national health care cost amounted to about $1.5 trillion or about 13% of the total GDP[5]. In the year 2017, the annual national health care costs rose to $3.5 trillion or 18% of the total GDP. Out of these, about 78% of the total cost account for chronic illness according to the World Health Organization. Moreover, only 5% of the chronically ill patients account for about 50% of the total healthcare expenditure, which is worrisome. The high cost for healthcare along with aging population is an alarming trend.

Hence, there is dire need to investigate and innovate novel methods and technologies that would enable people to lead better and longer lives at an affordable cost. This holds especially true for the field of organ transplantation and tissue grafts due to the shortage of organ and organ donors. As per a recent report[6], there were 49 public tissue engineering based companies in the US in 2018. Out of these, 21 were in the commercial phase of development and had tissue engineered products in the market. These companies made around $9 billion in sales with their products. If private companies are included, then this would be a significantly higher value. According to a report by Coherent Medical Insights in 2017, the field of tissue engineering was expected to grow at a rate of 11.5% during the years 2018-2026. Hence, there's a lot of room for innovations and technology

development in the field of tissue engineering. This will help in building better products for the masses which will help in healthcare treatment and management.

1.2 Current Methods of Treatment

The current gold standard for treatment of organ failure is organ transplantation. The challenges associated with organ transplantation have already been discussed in section 1.1. Apart from organ transplantation, several other methods exist for tissue injuries and repair. Tissue injuries are usually treated with grafting of tissues. There are three types of grafts that are used in the clinic: allografts, autografts and xenografts.

Allografts refer to biologic tissues which are harvested from a genetically nonidentical individual of the same species and transplanted to a host (e.g., human to human). Autografts are tissues which are harvested from one place of an individual and implanted to another place in the same individual (e.g., ligament transplanted from leg to arm in the same human). Xenografts refer to the tissues harvested from a genetically different species and transplanted to another species (e.g., pigs to humans)[7].

Autografts are the gold standard in terms of grafting tissues. But, the main problem with them is the donor site morbidity and limitation in the amount of available tissue. Additionally, autografts are only applicable for some types of transplants and cannot be used for organ replacements. The major problems with allografts is the foreign body response and immune rejection by the body. Similar is the case with xenografts, which face even higher magnitude of immune rejection and foreign body response from the host body. This is also known as graft vs. host disease. Additionally, there is a risk of disease

transmission with allografts and xenografts. In terms of cost effectiveness, xenografts are least expensive, followed by allografts and then autograft procedures[8, 9].

These challenges can be overcome using natural biopolymers and by sourcing cells from the donor patients. In this way, the immune rejection and foreign body response can be brought to a minimum while still using exogenous materials. One other way to get around this problem would be to use cells and decellularized tissues from the body, eg. omentum[10] and extra cellular matrix (ECM)[11] and then utilize it to make organs[12]. Hence, it has become possible to fabricate tissues and organs from exogenous and endogenous materials.

1.3 Tissue Engineering

The field of tissue engineering was started in the 1980's and 1990's and has gained significant prominence since then. People had started to talk about making totally artificial organs and robots with biology and biologically safe materials from then on. Finally, the promises of science fiction has some form of scientific backing. Although, in reality, we are still pretty far from making totally functional artificial organs, but certainly, the dream of fabricating artificial organs from scratch with biologically relevant materials has come to fruition[10, 13, 14].

The basic idea behind the field of tissue engineering is to fabricate organs/grafts which can be implanted in place of diseased organs/tissues. Tissue engineered scaffolds have three main components (often referred to as the "tissue engineering triad"): cells, scaffold and bioactive factors[15, 16]. These components and their properties dictate

where the tissue engineered graft can be placed. Hence, several biological, biochemical, chemical and mechanical cues dictate the placement of the graft[17].

1.4 Material Selection and Fabrication Techniques for Tissue Engineering

The major design criteria for building scaffolds for tissue engineering are: (a) it should restore tissue function which means that it should have correct shape and size with appropriate mechanical properties (b) there should be interconnected porosity within the scaffold for cellular infiltration and tissue ingrowth and also for nutrient and waste transport within the scaffold (c) it should be biocompatible or bioactive, in that, it dictates the fate of the various growth factors and cells within the scaffold (d) It should be biodegradable without any toxic byproducts and the rate of degradation should match the rate of ECM reconstruction within the tissue[18, 19].

According to Williams Dictionary of Biomaterials, biocompatibility is the ability of a material to perform with an appropriate host response in a specific application. The biocompatibility of a tissue engineering scaffold or matrix for a tissue engineering product refers to the ability to perform as a substrate that supports the appropriate cellular activity, including the facilitation of molecular and mechanical signaling systems, in order to optimize tissue regeneration, without eliciting any undesirable local or systemic responses in the eventual host. The various factors that can facilitate tissue expression are controlling cell proliferation and differentiation, tissue morphology and architecture and contamination and maintenance of phenotype. The various issues present with integration with host are control of acute and chronic inflammation, immune system, angiogenesis

and revascularization, tissue proliferation and scarring. Keeping all these things in mind, an ideal scaffold using ideal materials is very difficult to make as all the tissues and organs are made from a variety of materials in a way that can be only formed inside a body due to different genetical, phenotypical, biophysical and biochemical cues that are presented inside the physiological system. Nonetheless, researchers have tried to use various materials and methods to fabricate scaffolds and devices which can be implanted inside the body.

A variety of synthetic and natural materials have been investigated for different types of tissues and pathologies[20]. Traditionally, three types of materials have been used as implants inside the body; metals, ceramics and polymers. The use of metals have been restricted at hard implant-based applications such as knee, hip, shoulder, replacements, plates and bolts for fracture and stents. Similarly, the use of ceramics has been restricted to hard implant-based applications such as knee and hip replacements. Polymers, mainly hydrophilic polymers are the main materials that have been used in the tissue engineering field. These hydrophilic polymers when mixed in water are called hydrogels. This includes both synthetic and natural polymers. The major reason for using hydrogels in tissue engineering is that they come closest to mimicking actual tissues. The water content in these hydrogels can be tuned easily. Since, body tissues are mostly made of water, hydrogels are the materials which come closest to mimicking body tissues[21, 22]. Additionally, hydrogels can be functionalized in several ways to change their behavior and can also made be made stimuli-responsive. Moreover, metallic and ceramic

nanoparticles can be added to hydrogels to fabricate nanocomposite hydrogels for tissue engineering applications.

Some of the common synthetic polymers that are used in the field of tissue engineering are alpha-hydroxy esters such as poly lactic acid (PLA), poly glycolic acid (PGA), poly lactic glycolic acid (PLGA), poly caprolactone (PCL), poly methyl methacrylate (PMMA), poly hydroxy ethyl methacrylate (PHEMA), etc[17, 20]. They are biocompatible and can be manufactured to have a wide range of degradation rates by modifying the molecular weight, polymer ratio and degree of crystallinity. Other synthetic polymers that have been used in tissue engineering are polyethylene glycol (PEG), Polyvinyl alcohol (PVA), poly glycerol sebacatate (PGS), Poly(N-isopropylacrylamide) (PNIPAAM), etc. PEG is blank slate polymer that is very biocompatible and is inert inside the body. Mechanical diffusion and stiffness from a PEG hydrogel can be controlled by adjusting the initial MW and the crosslinking density. PEG crosslinking can be performed under mild conditions which are benign to cells and proteins.

Some of the most common natural polymers used in tissue engineering are alginate, gelatin, collagen, hyaluronic acid (HA), fibronectin and chitosan[17, 20]. Alginate is an unbranced, linear, anionic polymer derived from seaweed and the molecular weight is usually between 30 -270 kDa. Chitosan is a cationic amino polysaccharide derived from chitin which is sourced from shells of crustaceans. The molecular weight usually ranges between 7-200 kDa. Collagen, HA and fibronectin are extracellular matrix (ECM) components. The molecular weight ranges for collagen is around 300 kDa, for HA, it ranges between 7-20 kDa, whereas for fibronectin the molecular weight is about 440

kDa. Gelatin is denatured form of collagen with a molecular weight between 5-100 kDa. The main advantage with natural polymers is that they have cell binding motifs which make them highly biocompatible.

The advantages of synthetic polymers is that many properties such as mechanical stiffness, degradation rate and polymer weight can be easily controlled. But the major disadvantage is that they are usually not biocompatible but rather bioinert. The main reason for this is that synthetic polymers are devoid of any cell binding sequence. This makes natural polymers more attractive for tissue engineering applications. All the natural polymers derived from proteins and/or ECM have cell binding motifs which help in the adhesion and proliferation of cells in these materials. But the disadvantage with natural polymers is that they are usually mechanically weaker compared to synthetic polymers and their properties cannot be tailored as easily as synthetic polymers. To get around this limitation, researchers have tried to mix the two or more different types of polymers to get a good balance of both biocompatibility and mechanical stiffness.

The fabrication or manufacturing techniques are also a very important factor that governs the activity of a scaffold[23]. The manufacturing techniques dictate the necessary design criteria in a designing a scaffold[17, 24]. Additionally, they are very important in terms of scaling up the process for commercialization of the scaffold. They are also essential for Current Good Manufacturing Practices (cGMP) manufacturing processes. Some of the traditional manufacturing methods that have been used for creating scaffolds are electrospinning, particulate leaching, phase separation and gas foaming. Electrospinning uses synthetic polymers in an organic solvent to spin fibers on a substrate.

Particulate leaching uses polymer and a salt emulsion, and the salt is leached through polymer-salt matrix after putting the matrix in water. Phase separation uses removal of the solvent through solvent evaporation or solvent separation (freeze drying is an example). In gas foaming, a gas forming agent is mixed with the polymer and is released from the polymer matrix by elevating the temperature or the pressure (usually CO_2 gas is released from matrix). These fabrication strategies have been used majorly for synthetic polymers to create porous structures in the matrix. Although, these methods were fairly successful but had a number of limitations. In most of these processes, it's very difficult to include cells during the process in the matrix. Additionally, it's difficult to accurately control the pore size and mechanical strength of the matrices. Hence, it becomes imperative to use fabrication strategies that are more cell friendly and the properties of the scaffold can be controlled more precisely. In the past two decades, additive manufacturing or 3D printing has emerged as one of the emerging areas to precisely make parts and with great accuracy and detail. As a result, bioengineers have also applied 3D printing techniques to fabricate tissues and scaffolds.

1.5 Additive Manufacturing for Tissue Engineering

In the past decade, great progress has been made in the field of additive manufacturing[25, 26]. As a result, additive manufacturing has been applied in the field of tissue engineering. Additive manufacturing is the deposition of material in a layer by layer manner. When layer by layer deposition of material is done in the z-axis along with cells, it is known as bioprinting or 3D bioprinting. In the last decade, a vast number of

materials have been screened for bioprinting and a variety of methods have been developed for bioprinting applications. The ease of application of additive manufacturing and the precise control of material deposition makes it a very promising technology for tissue engineering. The porosity and mechanical properties of the printed scaffold can be controlled very easily.

Through 3D bioprinting, cells, biomaterials, and bioactive molecules are positioned with precise spatial control in a layer-by-layer fashion. With this technology, it is possible to engineer 3D tissue constructs with specific geometries and heterogeneities and, therefore, to mimic the in vivo counterparts in terms of both structures and functionalities. Human scale cartilaginous tissues/organs have been created to a very high resolution using natural polymers with additive manufacturing technologies. This was not possible with any other fabrication technology that were conventionally used for tissue engineering. Hence, it is a very promising and enabling technology for tissue engineering application.

Although, bioprinting is an enabling process, it comes with its own set of technical challenges. Some of the main properties to keep in mind for bioprinting applications are: (a) printability of the ink, (b) good biocompatibility during and after the printing process (c) ideal degradation kinetics and byproducts of the printed structures (d) ideal structural and mechanical properties of the printed structure (e) structural and functional similarity to the actual organ. Hence, it is very important to consider these factors and design the experimental study in a way that it incorporates all these factors to make a scaffold that can be actually placed inside the human body and hence translation of the technology can

be easily achieved. More will be discussed about additive manufacturing technology in the second chapter.

In the past decades, animal models and two-dimensional (2D) cell culture validation methods have been widely used in disease studies and drug discovery. However, animal models poorly mimic the underlying mechanisms in humans and tend to lead to ethical problems, while 2D culture methods have failed to reproduce the microenvironment and recapitulate the organ level physiology properly. Therefore, the demand for more accurate three-dimensional (3D) in vitro models arose and the concept of organs-on-chips was introduced.

Apart from additive manufacturing, microfluidic device technology has also been developed in the past two decades for modelling human tissues. A variety of on-a-chip devices such as different organ-on-a-chip, vasculature-on-a-chip, disease-on-a-chip have been fabricated and shown good efficacy in modelling behavior of different human tissues/organs. The main advantage with microfluidic technologies is that it can be made in micron scale and continuous perfusion can be achieved in these devices. The possibility of continuous perfusion allows cells to grow and proliferate in dynamic conditions rather than traditional static conditions. This makes microfluidic technologies a very promising technology to apply in the field of tissue engineering. More will be discussed about microfluidic devices in the second chapter.

1.6 Research Objective

With the growing need for tissue and organ replacements due to the aging population and a variety of diseases, the gap between the organ donors and patients waiting on the waitlist is constantly rising. Hence, there is a huge need for fabricating synthetic tissues and organs that can either be implanted inside the body or can be used for the testing drugs. This has resulted in extensive research over the past 2-3 decades in the field of tissue engineering (TE). As a result, a wide variety of materials and fabrication techniques have emerged for tissue engineering applications. Additive manufacturing and bioprinting have emerged as a very powerful fabrication technique for printing synthetic tissues and organ due to its high precision of depositing material and to print complex structures. Extrusion based printing is one of the most common 3D printing techniques for TE. A lot of research has been conducted on various materials for different TE applications. The work in Dr. Akhilesh Gaharwar's lab at Texas A&M University is focused on hydrogel-based nanomaterials for tissue engineering applications. Mainly, we have worked a lot with Laponite based nanoparticles for tissue engineering applications[27]. We have applied these nanoparticles for the development of bioinks apart from a variety of applications[28-30]. This work is based on Laponite XLG nanoparticles for additive manufacturing applications.

The objective of this research is twofold: The first aim is applying Laponite XLG nanoparticles for printing in support bath and the second aim is to use Laponite XLG as sacrificial inks for hydrogel-based microfluidics. To this end, first, different concentrations of Laponite XLG are examined for their printability. Then, Laponite XLG

is used as a support bath to print or extrude materials inside this colloidal solution. Next, we print Laponite XLG on top a cast gel and use it as a sacrificial material for making channels inside a hydrogel based microfluidic device.

CHAPTER II

BACKGROUND AND LITERATURE REVIEW

2.1 Rheology and Viscosity

Rheology is derived from the Greek words “Rheo” = flow and “logy” = study. So, rheology means the study of flow and deformation of matter. The matter in concern could be liquid or solid. Flow is the constant deformation of fluid when a force is applied to it. A liquid tries to relieve the strain applied by any force by flowing (straining) corresponding to that force. The resistance provided by the liquid on application of force is called the viscosity and it is the most relevant term when discussing about rheology. The viscosity of a material is inherent to the material which is based on the intramolecular forces inside the material. The definition of viscosity can be given by the parallel plate flow experiments. This experiment was first conducted by Sir Isaac Newton. In this experiment, a fluid is kept between two parallel plates and one of the plates is moved parallel to the other which is kept static.

Shear stress and shear rate are the common terms are used in describing the flow behavior. Shear stress (τ) is the force (F) applied by the rectangular moving plate with area (A) and shear rate (γ·) is the change of velocity (v) with respect to the vertical distance (x) from the surface. So, shear stress and shear rate are written as:

$$Shear\ stress\ (\tau) = \frac{F}{A}\left[\frac{N}{m^2} = Pa\right] \qquad \text{Shear rate } (\gamma\cdot) = \frac{\mathrm{v}}{\mathrm{x}}[\mathrm{s}^{-1}]$$

Then, viscosity is calculated by the given equation:

$$\text{Viscosity} = \frac{\tau}{\dot{\gamma}} [\text{Pa s}]$$

The above equation holds true only for Newtonian fluids but fails for other types of viscoelastic fluids. Most fluids don't exhibit Newtonian behavior and come under the category of Non-Newtonian fluids. The most popular and convenient method to check for rheological properties is a rheometer.

2.1.1 Types of Fluid flow

Fluids can exhibit mainly two types of flow behavior: Newtonian and Non-Newtonian fluid flow. Newtonian fluids experiences shear stress that is linearly correlated to strain rate or the viscosity of the fluid does not vary with strain rate. Conversely, for Non- Newtonian fluids, the viscosity is not linearly correlated to strain rate, or the viscosity of the fluid varies with strain rate. There can be different types of Non-Newtonian fluid flow behaviors: shear thinning (pseudoplastic), shear thickening (dilatant), Bingham plastic. Shear thinning fluids have a decrease in their viscosity when the strain rate is increased. Ketchup and toothpaste are examples of shear thinning fluids. On the other hand, shear thickening fluids have an increase in viscosity with increase in the strain rate. Corn starch in water or Oobleck is an example of shear thickening fluid. Bingham plastics can be Newtonian or shear thinning fluids, but they require a certain yield stress to start flowing. Ketchup and clay suspensions are examples of Bingham plastics. Time dependent non-Newtonian fluids can be categorized into two categories: thixotropic and rheopectic. In thixotropic fluids, the apparent viscosity decreases with duration of stress and in rheopectic the apparent viscosity increases with duration to stress.

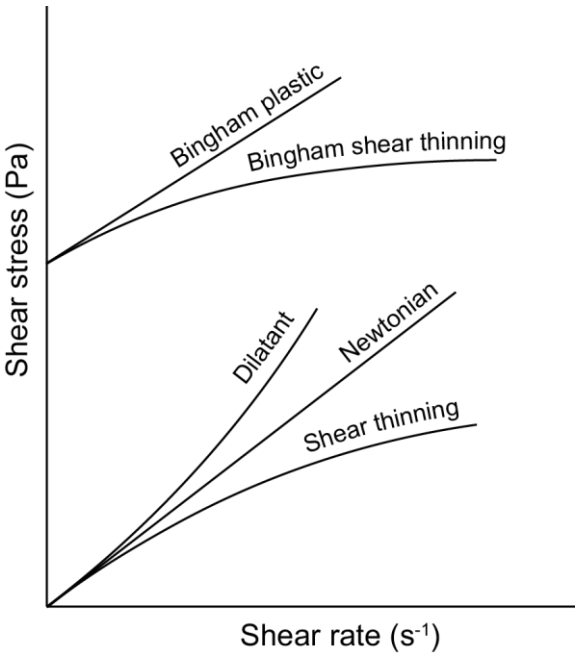

Fig. 2.1 Graph showing the various types of time independent fluid flow behaviors.

2.1.2 Types of Rheological Modifiers

There are various types of rheological modifiers that are used in the industry to modify the rheological behavior of a fluid. Modifying the rheological behavior can be useful for processing and storage. They can also change the overall quality and feel of the formulation. For a formulation, the rheological properties can be modified by changing the concentration and the compositional makeup that might contain pigments (organic, inorganic), binders (polymers, oligomers, reactive diluents), fillers, additives (stabilizers, initiators, catalysts, etc.) to modify the behavior of the fluid. Additionally, the properties

of the modifiers vary over time. Hence, rheological modifier selection is very important, and a number of properties need to be known for finding the correct polymer.

Rheological modifiers can be of two types: organic and inorganic. Organic rheological modifiers are more diverse compared to inorganic modifiers. They can be naturally or synthetically sourced. Polysaccharides such as cellulose, xantham gum, and carrageenan are common types of natural rheological modifiers while poyacrylamides or polyurethanes are the common synthetic rheological modifier. The synthetic modifiers can be subdivided into associative and non-associative rheology modifiers. Associative modifiers consist of non-specefic interactions of hydrophobic end groups of a modifier molecule both with themselves and the solvent. Non-associative modifiers function via entaglements of soluble, high molecular weight polymer chains and the degree of rheological modification is governed by the molecular weight of the polymer. attapulgite clays, bentonite clays, organoclays and treated and untreated synthetic silica clays are the most common types of inorganic rheologic modifiers.

Rheological modifiers can also be grouped according to their solubility in the solvent, ie, water based or solvent based. organoclays, hydrogenated castor oils, fumed silicas or polyamide are solvent-based modifiers whereas natural polysaccharides like cellulose, acrylic thickeners, associative thickeners. The focus in this study is on a water based inorganic clay rheological modifier called Laponite and the following discussion will be focused on that.

2.2 Description of Laponite

Laponite (also known as nanoclay) is a synthetically produced two-dimensional layered clay. It is synthesized from inorganic mineral salts and is manufactured and sold by a company called BYK additives. It is a disc shaped nanoparticle with 20-50 nm in diameter and 1-2 nm in thickness[27]. The empirical formula for Laponite is $Na^{+0.7}[(Si_8Mg_{5.5}Li_{0.3})O_{20}(OH)_4]^{-0.7}$ and it is characterized by its unique charge distribution. It has negative charges on the faces and partial positive charges on its edges which imparts unique properties to the nanosized particles. The density of Laponite is about 2.57 g/cm^3 and its specific surface area is about 370 m^2/g. Industrially, it's used as a rheological modifier in a variety of applications such as toothpaste, cosmetic products, cleaning products, paints, coatings and sprays.

As per Neumann, 1971[31], Laponite is manufactured by slow combination of magnesium salt, acid sodium silicate, sodium carbonate in a controlled temperature, pressure and shear rate to form an aqueous slurry. This slurry is then hydrothermally treated for about 10 to 20 hours to crystallize the synthetic clay. The resulting cystallized clay is washed and dewatered and then dried at a temperature of about 450° C to get a fine white powder of clay. Laponite is composed of various layered structures of octahedral magnesium and lithium ions sandwiched between tetrahedral silicon ions. There are 10 different grades of Laponite that are sold by BYK Additives, based on different stoichiometry of metal content in them and the application that they are used for. Laponite products can be loosely categorized into two basic grades: gel forming grade and sol forming grades. Gel forming grades of laponite form clear, colorless, high viscosity

colloidal dispersions when dissolved in water. Sol forming grades of laponite have the same dispersion characteristics. The work done is this thesis is mainly based on Laponite XLG, hence all further discussion will be based on Laponite XLG.

The composition of Laponite XLG is oxygen (62.34%), silicon (20.78%), magnesium (14.29%), sodium (1.81%), and lithium (0.78%) as verified validated experimentally via inductively coupled mass spectrometry (ICP-MS). Laponite is dissolved in deionized water to form a colorless, clear colloid viscoelastic gel. Depending on the concentration of Laponite in water, it forms a viscoelastic sol or a gel. The isoelectric point of Laponite is about pH=10 and it starts to chemically dissociate at pH lower than 9. The dissociation products of Laponite have been shown to be non-toxic ions such as Na^{+}, Li^{+}, Mg^{2+}, and $Si(OH)_4$ below pH=9. Due to its high surface area, unique charge distribution, size and low toxicity; Laponite has been investigated extensively in the tissue engineering field to make nanocomposite hydrogels[32, 33]. It has shown efficacy in the osteogenic and chondrogenic differentiation of stem cells and has been investigated for osteochondral tissue engineering. It has been investigated as tissue adhesive, surgical glue, sealant, hemostat, embolization gel, immunomodulative agent and for 3D organoid culture. Additionally, it has also been extensively investigated as a drug delivery agent[27]. In the past decade, it has been added to bioink formulations to aid the printability of different soft material based inks for additive manufacturing applications. The ability to impart shear thinning and thixotropic behavior makes it a very promising additive to hydrogel based inks. The following discussion and work in this thesis would be based around the use of Laponite for additive manufacturing applications.

2.3 Additive Manufacturing and Bioprinting

Additive manufacturing is the layer by layer addition of material as described before in section 1.3. This technique has been applied and researched extensively in the past decade in the tissue engineering field. A variety of materials have been investigated and continue to be investigated. The widespread use of additive manufacturing in tissue engineering is due to the ease of use, precise control to deposit material, possibility to add cells inside the ink before and during printing, and relatively biocompatible processing of materials during the whole process. There are many different types of additive manufacturing techniques that have been explored by the researchers. When material is added layer by layer along with cells, the process is called as bioprinting and the material used is called bioink.

The four main different types of bioprinting processes are: inkjet, laser assisted, stereolithography; and extrusion bioprinting[26, 34]. Inkjet bioprinting uses thermal or piezoelectric actuators to effect drop of liquid inks. The major advantages of inkjet bioprinting are fast fabrication speeds, high resolution, low cost, and ability to print low viscous materials. The major disadvantages are low cell density, inability to print tall structures, and inability to print high viscous materials. Laser assisted printing involves the use of laser to use and sacrificial layers to deposit bioinks. The major advantages are high resolution, deposition of biomaterials in solid or liquid phase while the major disadvantages are high cost, and thermal damage due to nanosecond/femtosecond laser irradiation. Stereolithography bioprinting requires the use of UV or near-UV light to crosslink a structure immersed in a pool of bioink or resin. The advantages of this type are

nozzle-free technique, printing time independent of complexity, high accuracy and cell viability but the disadvantages are damage and toxicity of cells by UV and near-UV light and inability to print multi-cell structures. Finally, extrusion based bioprinting involves the use pneumatic or pressure-based extruder to push the bioink through a small needle. The advantages of extrusion based bioprinting are its relative ease of use, capability of printing various biomaterials, ability to print high cell densities and its disadvantages are relative slow speed and inability to print low viscous materials. Comparing the pros and cons of different processes, it turns out that extrusion bioprinting is the most relevant method for printing a wide variety of materials[35]. Due to its versatility, low cost and ease of scalability, it has become the most ubiquitous process to be adopted by biomedical researchers around the globe. One of the most important requirements for the material to be extruded is its ability to show shear thinning behavior and quick thixotropic recovery. Hence, we have Laponite in this study since it shows the properties.

2.3.1 Traditional Bioinks vs. Advanced Bioinks

Apart from the type of process and parameters, material selection is the most important yet limiting factor for bioprinting. The material that is extruded is called bioink (for bioprinting) or just ink (for non-bioprinting applications). It's imperative for a bioink to be printable and show good cell viability at the same time. Some of the controllable properties of a bioink for extrusion bioprinting include viscosity, shear thinning, thixotropic recovery, biocompatibility, viscoelasticity, gelation kinetics, biodegradation and hydration degree[36]. Hydrogels are a class of hydrophilic polymers that swell upon

contact with water[15]. Their ability to most pertinently mimic the native tissue environment compared to any other materials makes them suitable candidates for tissue engineering and bioprinting[37, 38]. Since cell viability is one of the most essential requirements, natural polymers such as chitosan, alginate, gelatin, collagen, agarose have been studied as they are readily cytocompatible and biocompatible, compared to their synthetic counterparts[39]. Traditionally, single-component hydrogel bioinks have been investigated for bioprinting applications but they lack in many departments to be considered as suitable candidates for ideal bioinks. Generally, they have shown to possess poor printable properties. To compensate this, the polymer concentration and crosslinking density is increased which reduces the cytocompatibility of these inks. To circumvent the inherent limitations associated with single-component hydrogel bioinks, advanced bioinks have been proposed. The so called advanced bioinks can be classified into four major categories: multimaterial bioinks, supramolecular bioinks, interpenetrating networks (IPNs) bioinks and nanocomposite bioinks[36]. Multimaterial bioinks, as the name suggests, consist of multiple materials such that one component supplements the properties of another component. For eg, Hyaluronanic acid methacrylate (HA-MA) and gelatin methacrylate (GelMA) were mixed to print trileaflet heart valves[40]. While GelMA enhanced cell viability, HA-MA increased the viscosity and stiffness of the resulting bioink. IPN materials, unlike multimaterial bioinks are polymer networks that are physically entangled but are separately covalently crosslinked on their own. They involve the use of elastic and flexible polymer at a high concentration and a stiff and brittle polymer at a much lower concentration[41, 42]. These bioinks have shown to have

increased stiffness and fracture strength compared to individual components. Supramolecular bioinks are composed of short repeating units with functional groups that can interact non-covalently with other functional units, forming large, polymer-like entanglements. Under high stress, these non-covalent bonds are reversibly broken to dissipate energy. The reversibility of these bonds also leads to shear-thinning properties that facilitate their use in bioprinting. Lastly, nanocomposite bioinks use nanomaterials in polymeric hydrogels to provide needed functionality in the bioink. They can also be incorportated to functionalize bioinks with better mechanical properties, shear thinning behavior, biocompatibility, electrical conductivity, magnetism, etc. Polymeric hydrogels incorporated with laponite nanosilicates have been investigated in the Gaharwar lab and other groups as bioinks. In addition to imparting shear thinning behavior, Laponite nanodiscs also provide high cell viability due to lower shear forces experienced by cells.

2.3.2 Sacrificial Support Bath 3D Printing

Traditionally, extrusion-based printing of soft materials like hydrogels only included solid freeform fabrication or printing on a bed with air as the medium. The main challenges with this type of printing is the limitations in printing in the z-axis(height) and to print overhangs. But over the last five years, various researchers have investigated layer by layer printing inside a viscous liquid medium[13, 43-52]. The viscous medium allows the structures to be printed in a z-direction with good resolution and to print overhangs inside the bath. One other advantage of printing in a support bath is that low viscous inks can also be printed with ease inside a support bath.

The basic idea behind support bath printing is to extrude material in a viscous medium rather than in air. This support bath material should be viscous with shear thinning and thixotropic properties. The shear thinning properties with a yield stress liquify the material near the nozzle tip and lets the nozzle tip to extrude material in the medium easily. Additionally, the support medium should also be thixotropic which means it should quickly rebuild itself in the nozzle's wake after the ink from the nozzle has been extruded to keep the material in place. If the support material in not thixotropic, the extruded material will not stay in place and flow in the medium. In other words, the extruded material is jammed in its place by the support material. In traditional extrusion printing in air, surface tension and gravity are the limiting factors for giving a high-resolution print. Surface tension tries to make the filament diameter to a small spherical area to lower the energy and gravity weighs down the extruded filament[44, 49]. The use of a support bath negates these two limiting factors as extruded material faces negligible surface tension as both the mediums are visoelastic gels (or liquids) and since the support bath supports the print, it balances the force of gravity, hence gravity doesn't affect the print[44].

Researchers have used different materials such as gelatin microparticles, hydrogels, varieties of Carbopol and Laponite for support bath printing[13, 48, 53]. Each material has their own advantages and disadvantages. Recent research has also used more biocompatible natural materials as support bath for tissue engineering applications. We used Laponite in this study because of its advantages over other materials[51] and our previous experience with it. We have used a combination of Gelatin methacryloyl (GelMA) and Kappa Carageenan (KCa) as our ink formulation due to the good

biocompatibility of the ink and previous use for extrusion based bioprinting in the Gaharwar Lab. GelMA provides cell binding motifs and chemical crosslinking sites in the matrix whereas KCa is used as a rheological modifier which makes the whole formulation shear thinning and allows for easy extrusion.

2.3.3 Sacrificial Inks for Hydrogel-based Microfluidics

Microfluidic technology to recapitulate the human organ systems has become very promising in the past two decades[54-57]. The main advantage is that perfusion of different media, nutrients and gases can be achieved very easily which makes it a dynamic system, compared with the traditional tissue engineering applications. The dynamic behavior is closer to physiological systems compared to the static systems. Different systems such as organ-on-chip, vasculature of chip, disease on a chip have been investigated. Conventionally, polydimethylsiloxane (PDMS) and polycarbonate have been used for making these devices. The limitation of these materials is that they are inert materials and show weak permeability and biocompatibility. Cells must be within 100-200 um near blood vessels or capillaries to grow and survive or necrosis takes place in an engineered tissue. Hence, it becomes very important to use hydrogels for making microfluidic devices[54, 58, 59]. Recent research has investigated the use of hydrogels for making microfluidic devices. Specifically, some of the natural and synthetic polymers, such as agarose, gelatin, alginate, collagen, and cross-linked PEG have been used[60].

In terms of fabrication methods, layer by layer assembly of hydrogel sheets,

sacrificial template technology and 3D bioprinting have been used. Layer by layer assembly has problems of bonding the hydrogel layers together. Sacrificial templating usually requires harsh postprocessing methods. In this study, we have investigated the use of Laponite as sacrificial ink for making microfluidic channels. We have used extrusion based additive manufacturing to deposit the layers of sacrificial Laponite. There are many advantages of using Laponite: (a) it is very easy to use for 3D printing applications and can print channels of desired shape and size (b) it is cost effective (c) it requires very gentle postprocessing to remove the sacrificial laponite layer. For the hydrogel system, we used a mixture of gelatin and GelMA as gelatin can be physically crosslinked whereas GelMA can be chemically crosslinked which is helpful in mechanical integrity of the microfluidic devices.

CHAPTER III

MATERIALS, EXPERIMENATAL METHODS AND RESULTS

3.1 Qualitative Assesment of Viscosity of different Nanoclay concentrations

The first experiments were done to characterize the properties of different concentrations of Laponite powder in Deionized (DI) water. Laponite concentrations were varied from 1% w/v in DI water to 10% w/v with concentrations increasing by 1% w/v. Laponite was purchased from BYK Additives. Laponite gel formulations were made by

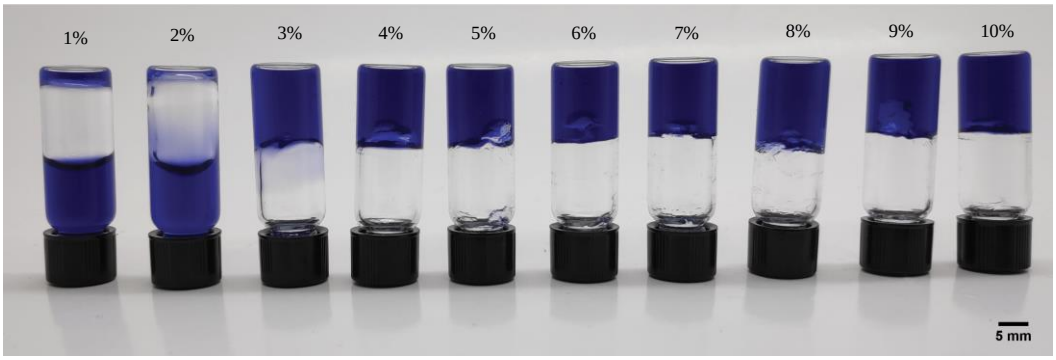

Fig. 3.1 Inverted vials show the viscosity of different concentrations of Laponite XLG gels, 24 hrs after exfoliation. Scale bar: 5 mm

adding the desired amount of Laponite powder in DI water, vortexing them in a vortex shaker for 2-5 minutes and letting the Laponite exfoliate for 24 hours. Exfoliation means the dispersion of Laponite discs from the tactoid stacked geometry to individual particles in water. This happens by the release of Na^+ ions that are present between the laponite disks. Initially, qualitative experiments were done to check the flow of Laponite gels after

24 hours. The different laponite concentration gels were made in small vials and turned upside down after 24 hours (Fig. 3.1). Blue food coloring was used to aid the visibility of different gels.

3.1.1 Results

The viscosity of the concentrations from 3% and above w/v Laponite concentrations formed a gel which could support their own weight but 1% and 2% were still liquid enough to not be able to support their own weight (Fig. 3.1). Hence, they were deemed to be unfit for 3D printing.

3.2 Rotational Rheological Characterization of different Nanoclay concentrations

All rheological testing was performed with a stress-controlled rheometer (DHR-2 Discovery Hybrid Rheometer, TA Instruments, New Castle, Delaware) using 20 mm parallel plate geometry at a gap of 0.4 mm in conjunction with a solvent trap. All tests besides temperature sweeps were performed at room temperature to replicate the temperature of the ink inside the cartridge while being printed. Different concentrations of Laponite gel were prepared and exfoliated as mentioned in the last section. Rotational rate sweeps were performed on the different laponite concentrations from 1-10% w/v by varying the shear rate from 0.1-1000 s^{-1}. The viscosity was plotted with respect to (w.r.t.) shear rate (Fig 3.2(a)). The power law model was fitted on the obtained data and variables n and k were calculated. The shear-thinning index is determined by power law fitting of the viscosity vs shear rate curve as described in eq. $\eta = K\dot{\gamma}^{n-1}$ where η is the viscosity, K is the flow consistency index and n is the shear thinning index. Peak hold tests were

performed to mimic the behavior of the material inside the nozzle (Fig. 3.3(a)) by applying high shear rate (3000 s^{-1}) for 5 seconds which mimics the shear rate experience by the ink inside the nozzle and then negligible shear rate once it comes out of the nozzle. Viscosity and shear rate w.r.t. time plotted (Fig 3.3(b)). The time to recover to 80% viscosity was manually calculated as to qualitatively measure the thixotropic behavior of the ink. The plots for some of concentrations were removed from both Fig 3.3(b) and Fig 3.2(d) to make the graphs clear and legible. Similarly, to peak hold tests, multiple peak hold cycles were applied to see if the break and recovery can happen over multiple cycles. The shear rate applied was 3000 s^{-1} for a period of 5 s followed by a negligible shear rate = 0.02 s^{-1} for a period of 240 s. This was done for four cycles.

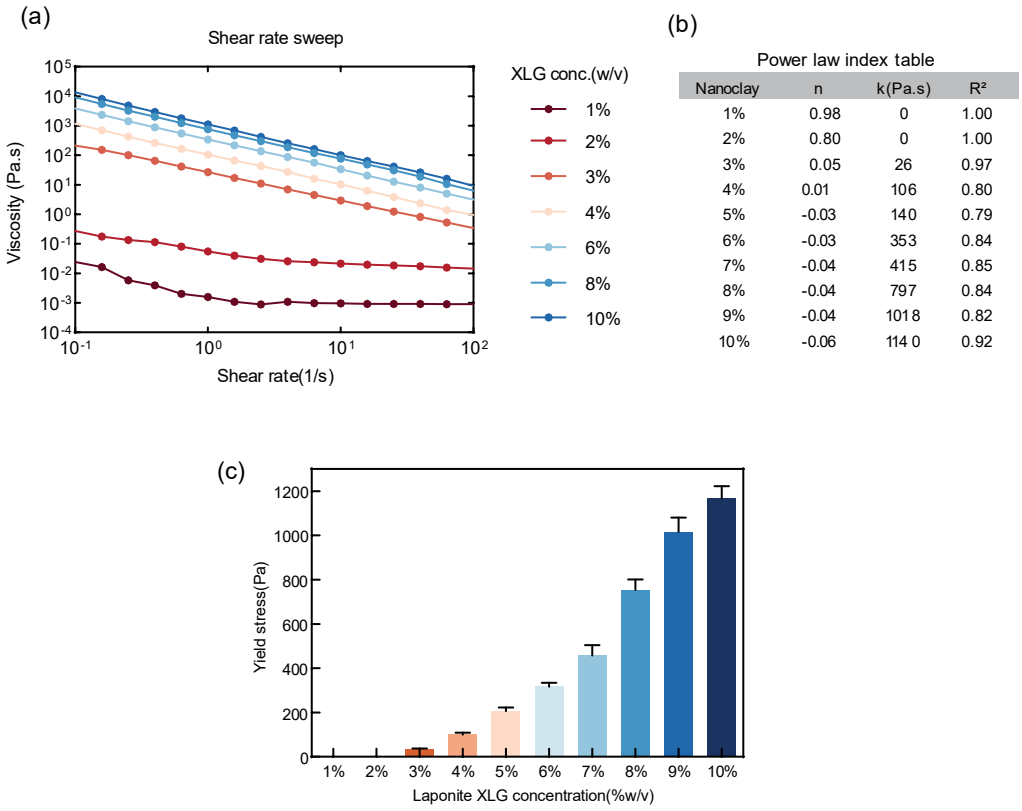

Fig. 3.2 Rotational rheological characterization. (a) Shear rate sweep on different concentrations of laponite and corresponding (b) power law index table beside the graph (c) Yield stress of different concentrations of Laponite XLG

3.2.1 Results

The shear rate graph shows that with increase in the concentration of Laponite, the shear thinning behavior of the ink also increases. This can be seen from the graph as both 1% and 2% concentration don't show much shear thinning behavior. But concentrations from 3% and onwards shear thinning behavior is shown by the ink. In the power law index, when n =1, the flow is Newtonian; n<1, flow is shear thinning; n>1, flow is shear

thickening. It is clear from the values of n in the power law index table (Fig 3.2(b)), as the concentration of Laponite increases, the shear thinning behavior also increases. Hence, laponite is causing the shear thinning behavior. Also, the increasing K value suggests that with increasing Laponite concentration, the packing density of Laponite in the formulation goes up which increases the electrostatic interaction among different nanodiscs. It has been suggested before that when shear is induced, the laponite particles orient themselves parallel to the direction of flow. This causes the partial positive charges on the rim and negative charges on the face to interact with each other. The type of electrostatic interaction repels the particles from each other, giving rise to shear thinning behavior. The yield stress values were also found using fig. 3.2(b). Fig. 3.3(a) shows the yield stress values for different concentrations of Laponite. Next, the thixotropic behavior of the different concentrations of ink are measured using the peak hold tests (Fig. 3.2(c)). From the plots, 2% and 3% Laponite concentrations don't show very good thixotropic behavior needed for quick recovery of the deposited inks. We chose 80% viscosity recovery from its initial viscosity as a qualitative measure to measure the thixotropic recovery time. The 2% and 3% couldn't recover in 2 minutes but 4% had a 40 second recovery time, 5% had 14 sec, and 6% and above had a recovery time of less than 10 sec. Additionally, peak hold test was applied for multiple cycles to see the behavior of ink for multiple cycles. It revealed that after the first break in the of all concentrations from 3%-6%, the building of the internal structure remains the same for every subsequent cycle which indicates the thixotropic behavior of Laponite over subsequent cycles. In 5% and 6%, the equilibrium viscosity dropped to about 80% of the initial viscosity. For 4% Laponite concentration,

the equilibrium viscosity remained like initial viscosity and dropped to no more than 10% compared to the equilibrium viscosity.

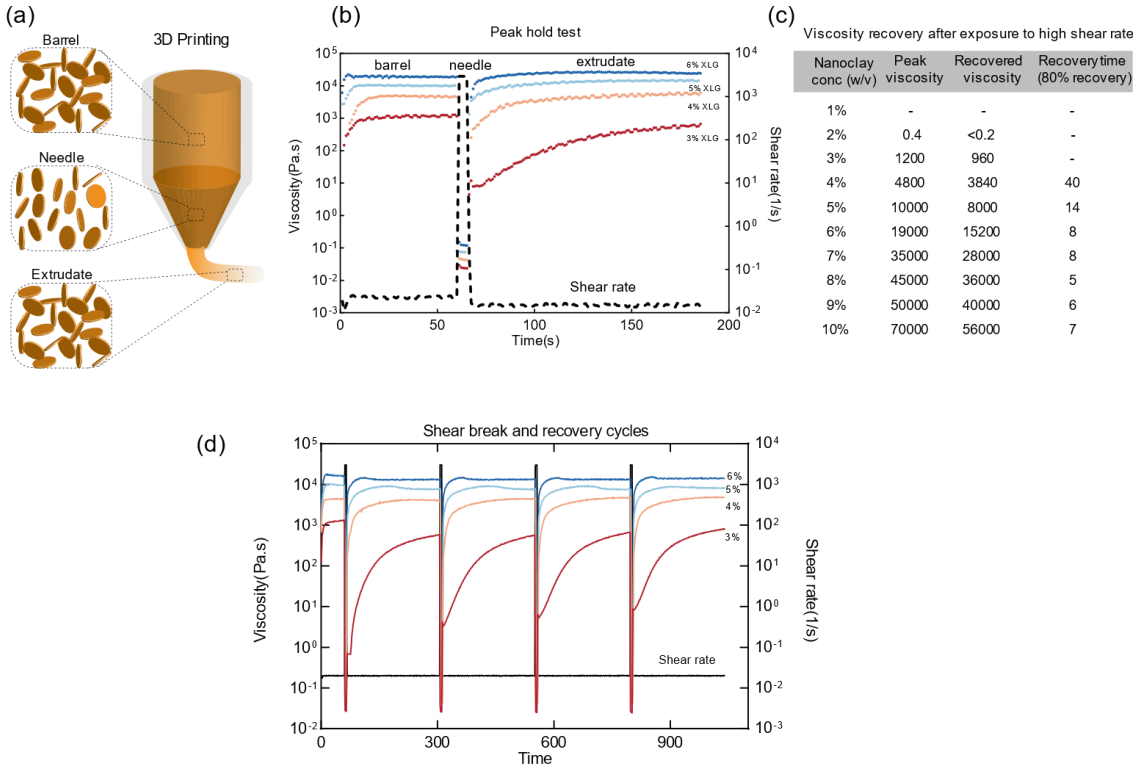

Fig. 3.3 Characterization of thixotropic behavior. (a) Schematic of Laponite ink in the barrel during extrusion of ink (b) Peak hold test of different Laponite concentrations and the viscosity recovery table beside it (c). (d) Peak hold test for multiple cycles.

3.3 Oscillatory Rheological Characterization

The oscillatory rheological measurements were also done on different Laponite concentrations. The aim of these experiments was to determine the storage modulus (G') and loss modulus (G'') over different frequencies, amplitudes and temperatures. We

performed these tests on Laponite concentrations from 3%-8% since it was clear that 1%,2% were not suitable for 3D printing and 9%-10% were very viscous and would aggregate into clusters. Only 4%,6% and 8% were plotted for better visibility and clarity. First, the amplitude sweeps were performed to verify the trends in yield stress obtained from rotational measurements. The amplitude was varied from 0.1-1000 Pa. Next, the frequency sweep was performed on the various concentrations. The frequency was varied between 0.01 Hz to 100 Hz. G' values at 1 Hz, 1 Pa from stress sweep and at 1 Pa, 1 Hz were plotted to see the trend in storage modulus. Also, crossover points from stress sweep were plotted to verify the yield points that were obtained from rotational sweeps. Moreover, temperature sweeps were performed to quantify the dependence of different concentrations on temperature. The temperature was varied from 25°C-85°C.

3.3.1 Results

The linear viscoelastic region was determined by Fig. 3.4(a). It was found that the crossover points (G'<G'') occurred at about 113 Pa, 341 Pa and 850 Pa for 4%, 6% and 8% Laponite concentrations. The yield stress trends were similar to that found with rotational tests. Next, the results of the frequency tests (Fig. 3.4(c)) showed the dependence of water w.r.t.frequency. As expected, it showed Newtonian behavior with G'

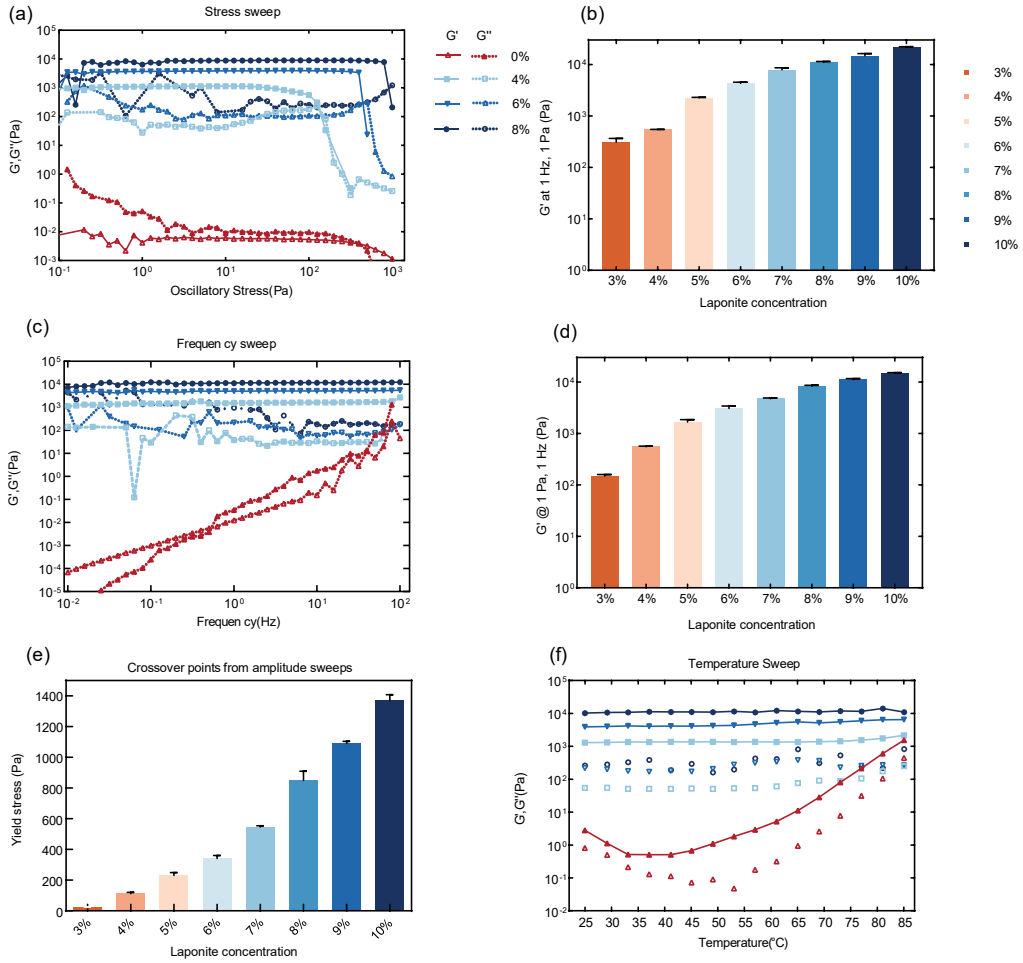

Fig. 3.4 Oscillatory sweeps of different Laponite concentrations. (a) Amplitude sweep from 0.1-1000 Pa (c) Frequency sweep from 0.01-100 Hz (f) Temperature sweep from 25°C-85°C to find the temperature dependence of Laponite.

and G" increasing with increasing frequency. In the case of Laponite formulations, their behavior showed that G' and G'' were independent of varying frequency, which indicated Non-Newtonian behavior. Internal structure formation with laponite addition seems to have quashed any dependence of behavior on frequency. After this, the temperature dependence of Laponite formulations were tested. As expected, due to evaporation of

water, the storage and loss modulus seems to rise with just water (Fig. 3.4(c)). But, in the laponite formulations G' and G'' remained constant over the temperature range of 25°C-85°C. This means that other polymers can be mixed with laponite and can be worked with higher temperatures without compromising the properties of the formulation.

3.4 Computational Fluid Dynamics (CFD) of different Nanoclay concentrations

Computational fluid dynamics simulation were performed on different concentrations of Laponite XLG in ANSYS Fluent. The values obtained from the rotational shear rate sweep by applying power law were input in the software. The inlet speed and minimum and maximum visocosity from the shear rate range were input in the software and simulations were performed. The simulations were performed on the outlet

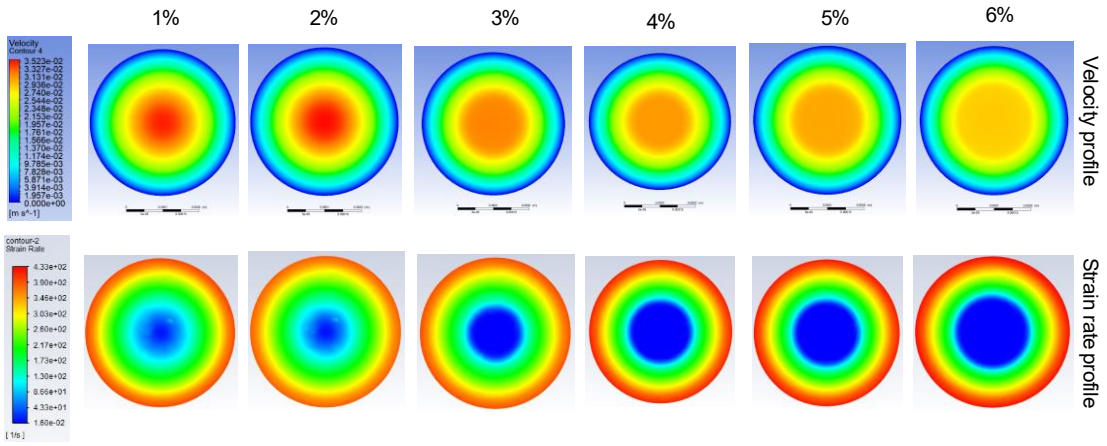

Fig. 3.5 Computational fluid dynamics (CFD) simulations of different nanoclay concentrations. CFD was done in ANSYS software. The circular rings represent the outlet of the nozzle. The top row represents velocity gradient with increasing concentrations while the bottom row represents the strain rate with increasing concentrations of Laponite XLG.

of needle as that's the regioin which is susceptible to most change in velocity and strain rate due to change in area of cross section of the needle.

3.4.1 Results

The results of the simulations (Fig. 3.5) show that as the viscosity of the formulations increase (increase in Laponite concentration), the gradient in the velocities and strain rates are lower for higher concentrations (4% and higher) compared to lower concentrations (3% and lower) of Laponite. This indicates that higher concentration of Laponite leads to plug flow behavior and the ink moves as viscoelastic solid while exiting the extruder tip. This can be good for cell shielding if the extrusion pressure is below the pressure detrimental for cell survival.

3.5 Characterization of different Nanoclay concentrations for 3D Printing

The commercially available thermoplastic extruder printer Anet A8 was modified to print hydrogels and soft materials. For this, the thermoplastic head was removed and a custom head for printing soft materials or hydrogels was made and put in place of the thermoplastic head. The control system was also replaced by changing the microcontroller and using the open source Arduino Uno microcontroller. All 3D designs were made in Solidworks and saved as .stl file. These files were exported to 3DSlicer which is an open source program. The 3DSlicer program cuts the design in layers that dictate the movement of different motors on the 3D printer. The slicer program generates G-code which is read by the 3D printer and dictates its movement. Another open source software called Repetier

(a)

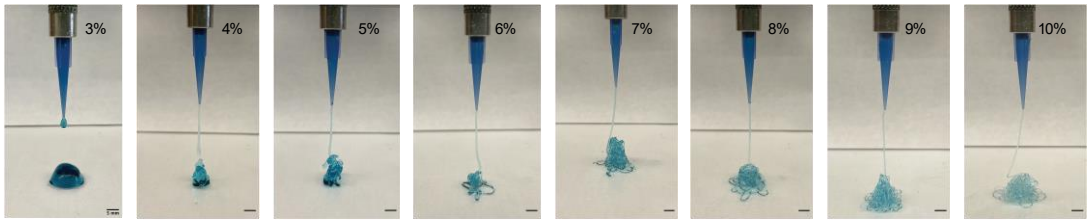

(b)

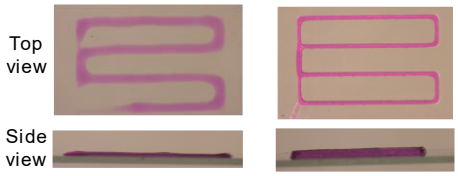

(c)

Normalized values - different dimensions(%)

Nanoclay (w/v%)	Width (1D)	Area (2D)	Volume (3D)
3	243	207	133
4	179	174	118
5	91	96	86
6	99	98	93
7	93	94	92
8	92	97	94
9	97	95	89
10	95	99	92

Fig. 3.6 Printing characterization of different nanoclay concentrations. (a) Extrusion of different concentrations of Laponite XLG from 2% w/v-10%w/v (Scale bar: 5 mm) (b) Top view and side view of 3% and 6% Laponite XLG printed in a simple line structure (Scale bar: 1mm) (c) Table showing normalized values, calculated in different dimensions width(from top), area(top lines) and volume(including the top area and side)

host was used as the interface for 3DSlicer. When printing on a hard surface in air, a 22 gauge plastic tapered needle was used. The printing speed was kept as 10 mm/s unless specified otherwise. The flow rate was 0.1 ml/mm. First, different concentrations from 3%-10% were extruded (Fig. 3.6(a)) with the extrusion speed mentioned above to look for the quality of the extrudate. Next, simple line structures were printed of Laponite concentrations between 3%-10% w/v to measure the precision of the printed structures compared to the actual model made in Solidworks. To quantify the precision, the prints

were directly compared, and the width, area and volume values were of the prints were normalized by that of the Solidworks model/computer design.

3.5.1 Results

Material selection and fabrication techniques for tissue engineering The extrusion tests (Fig. 3.6(a)) revealed that 3% and 4% concentrations were not able to print long continuous strands whereas concentrations of 5% and above formed long continuous strands which makes them favourable for 3D printing. Also, it can be seen in fig. 3.5(a) that 3% forms a pool of colloidal formulation with extrusion of droplet whereas other concentrations form continuous filament that can withstand their own weight. With simple lines being printed and quantified, the normalized values show that pooling of printed line occurs in 3% and 4% as their normalized values in all three dimensions were more than 100. It shows that these concentrations didn't hold their shape after extrusion and had a wide spread upon being extruded. Values of concentrations 5% and above showed that the strands did not spreading and the nanosilicates held water in their place as the normalized values were lower than 100 (Fig. 3.6(b) and 3.6(c)). Hence, concentrations from 5% and above were deemed fit for 3D printing. Since 6% had the best normalized values that were near 100, it was deemed to be the better concentration to 3D print structures.

3.5.2 3D Printing Complex Structures

With the same printing parameters as described earlier and 6% Laponite XLG complex structures of different shapes and sizes were printed.

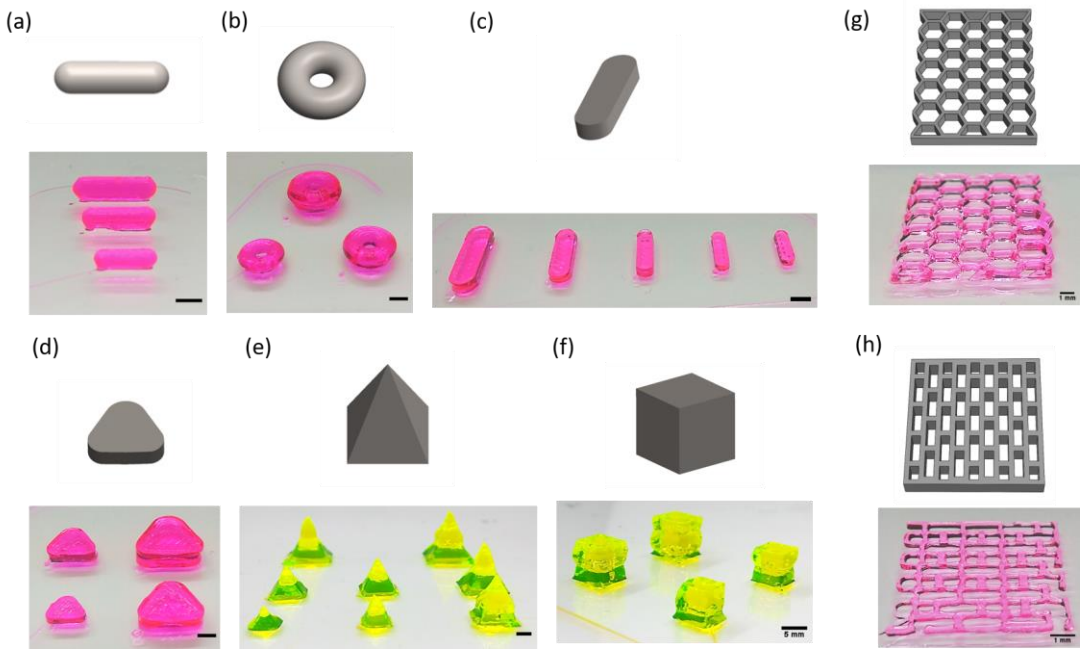

Fig. 3.7 Printing different types of shapes and sizes with 6% w/v Laponite XLG. The top row shows the Solidworks model while the bottom row shows the printed structure. From a-f (Scale bar: 5mm) and for (g) and (h) (Scale bar: 1mm)

3.5.3 Results

The printed structures held their shaped very well and 3D prints turned out to be to have good shaped fidelity (Fig. 3.7). The prints were very smooth, precise and they tended to be self-supporting their own weight. Although, the structures were printed very precisely, the structures didn't had any rigidity rather they were just gels. Rigidity and robust mechanical properties can be imparted to the structures by adding different types of water-based polymers in the formulation, printing it and crosslinking the structures.

3.6 Nanoclay as Sacrificial Support Bath for 3D Printing

Next, we used Laponite for support bath 3D printing applications. Support bath containing 4% w/v Laponite was made and used after 24 hours. 4% Laponite was chosen for the support bath as concentrations below 3% wouldn't form a viscous material to be used as a bath. We tested different laponite concentrations for support bath and found 3.5% and 4% formulations worked well for support bath printing. Concentrations above 4% didn't work well as they had a high yield stress and formed static crevasses at the wake of the translating nozzle which can be detrimental to printing inside the support bath[61]. This happens because the hydrostatic pressure at the printing depth is lower than the yield stress of the support bath. We used a combination of GelMA and KCa (10% GelMA, 0.8% KCa and 0.25% Irgacure 2959 (2-Hydroxy-4′-(2-hydroxyethoxy)-2-methylpropiophenone)). GelMA was used to since it can form a mechanically stiff polymer and has cell binding RGD motifs in the gel. RGD sequences promote cell adhesion and differentiation. KCa was used to make the formulation shear thinning. Irgacure 2959 was used as the photo initiator. The ink was mixed with either mixed with FITC/rhodamine to provide better visibility to the otherwise translucent ink. The same printer as described before was used for printing in the support bath. The movement of the printer was kept at 2 mm/s and the extrusion speed was 2 mm/s. 22 gauge metal needle was used for printing the different structures. After the structures were printed, the were exposed to a UV light at an intensity of about 30 mW/cm^2. Then, the printed structures were extracted out of the support bath by diluting the support bath with DI water/PBS.

Different designs such as bifurcated vessels, Texas A&M symbol, pancreas, femur, meniscus, DNA shape, heart, trileaflet valve were printed inside the support bath.

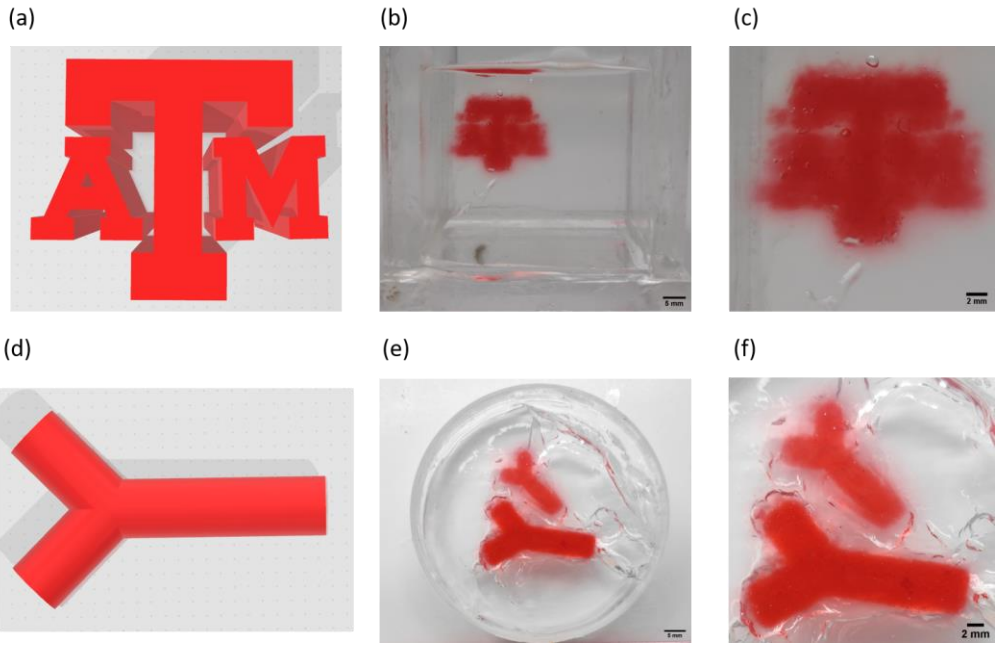

Fig. 3.8 Sacrificial support bath printing with nanoclay. (a) and (d) shows the stl file of Texas A&M logo and bifuracated vessel respectively. (b) and (d) shows the printed structure inside the bath. (Scale bar: 2 mm)

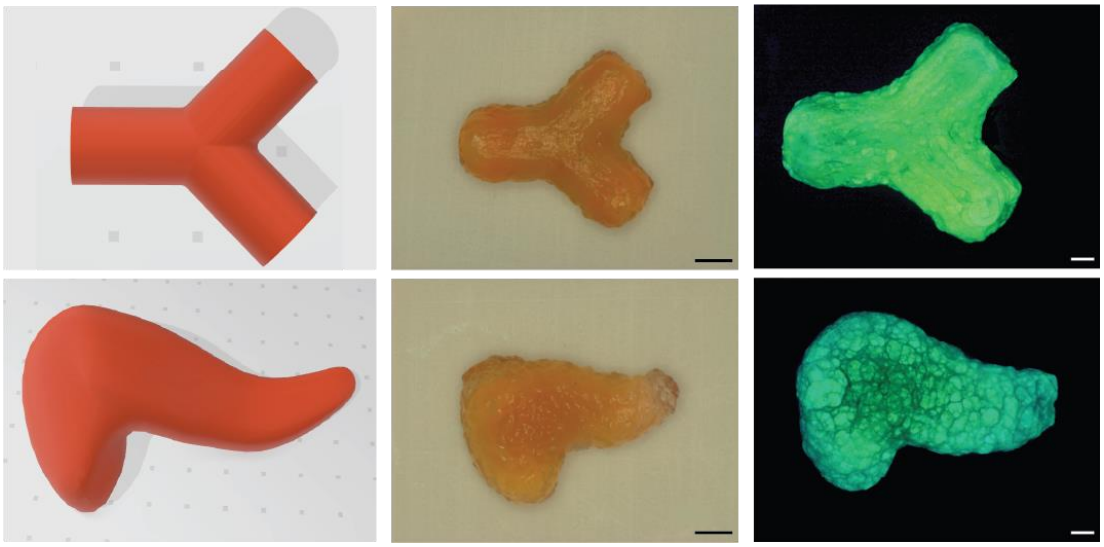

Fig. 3.9 Extracted printed structures. (a) and (e) - STL files for a Y shaped vessel and pancreas, respectively, (b) and (f) - images of corresponding 3D printed and extracted structures from the support bath, (c) and (g) - corresponding FITC fluorescent images of the extracted structures, (d) and (h) - inset of the fluorescent images (Scale bar: 2 mm)

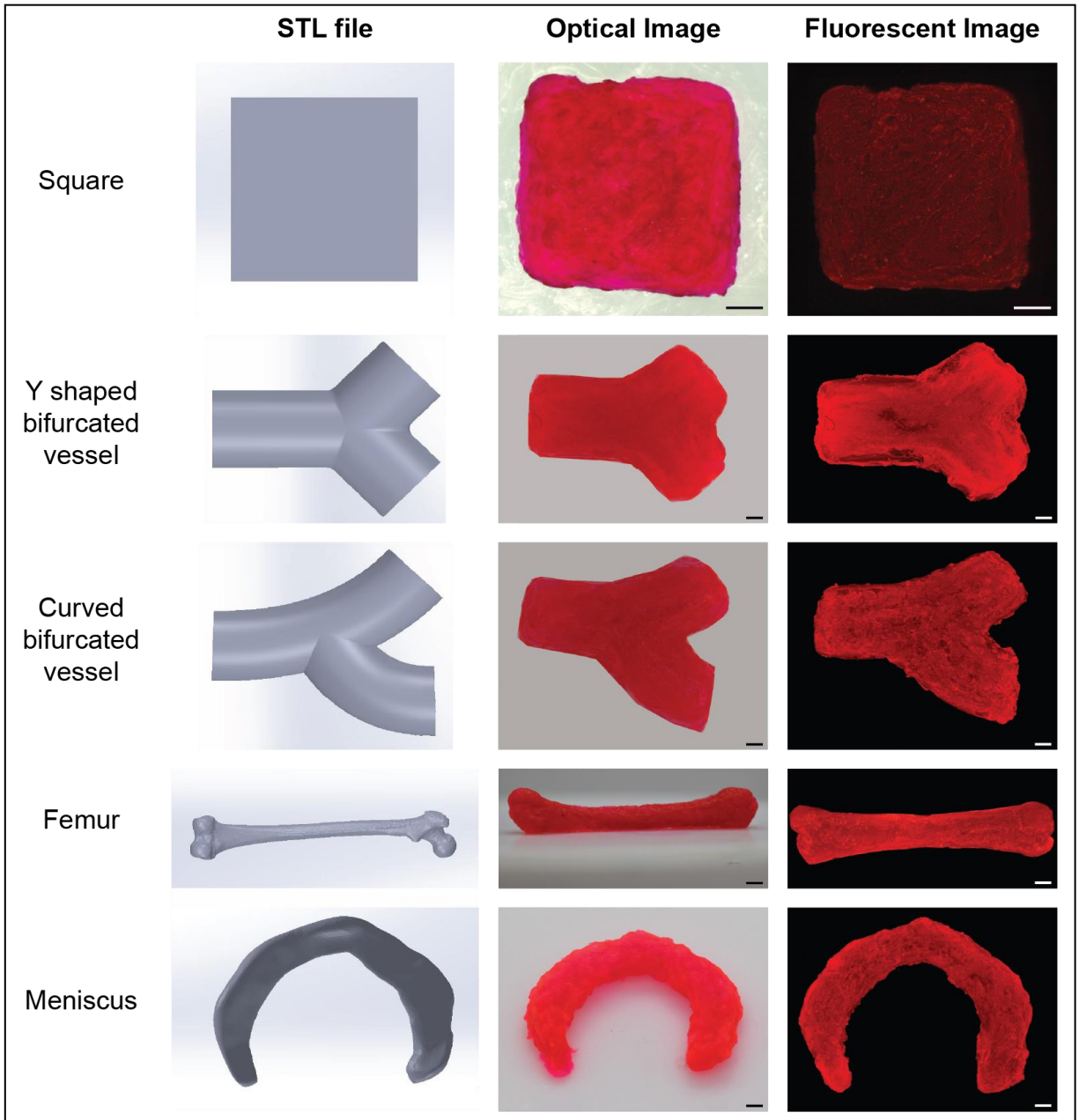

Fig. 3.10 Extracted printed structures from the support bath. The first column shows the stl file of the designs in Solidworks, the second column shows the brightfield imaging of the extracted prints and the third column shows the fluroscent imaging of the extracted prints (Rhodamine tagged). (a)-(c) Y shaped bifurcated vessel, (d)-(f) Curved bifurcated vessel, (g)-(i) Femur, (j)-(l) meniscus, (m)-(o) square. (Scale bar: 2 mm)

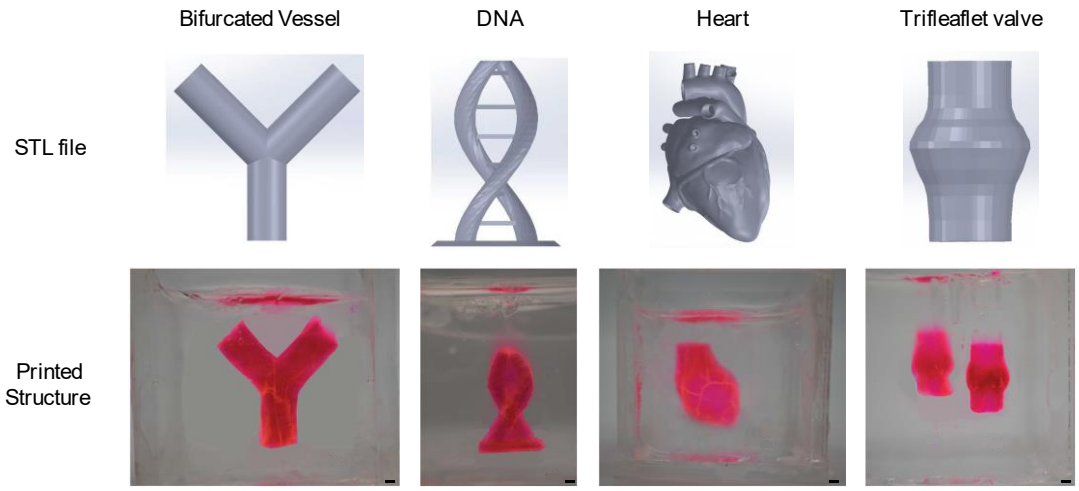

Fig. 3.11 Printed structures inside the support bath. Top row shows the stl files in Solidworks, bottom row shows structures printed inside the support bath. (a)-(b) Y shaped vessel, (c)-(d) DNA structure, (e)-(f) Heart, (g)-(h) Trileaflet valve. (Scale bar: 2mm)

3.6.1 Results

The different structures such as bifurcated vessels, Texas A&M symbol, pancreas, femur, meniscus, DNA shape, heart, trileaflet valve were printed inside the support bath. Fig. 3.8 and 3.11 shows the printed structure inside the bath and Fig 3.9 and 3.10 shows the printed structures that have been extracted from the bath. Structures in Fig 3.8 were tagged with a small amount of FITC/Rhodamine dye for fluorescent imaging. As it can be seen from the Fig. 3.7 and Fig. 3.8, the different structures that were printed and taken out of the support bath were comparable to the STL file and were able to be taken out of the bath. The Texas A&M symbol printed inside the support bath could not be crosslinked as the acrylic sheet from which the bath structure was made didn't allow UV penetration

through it and hence, it broke while it was being taken out of the bath. Other structures such as the two types of bifurcated vessels and pancreas were able to be UV crosslinked and they came out easily out of the support bath.

3.7 Nanoclay as Sacrificial Ink for Hydrogel-based Microfluidics

The next goal of the study was to test the feasibility of the Laponite as a sacrificial ink. For this purpose, a 5% w/v GelMA and 5% w/v Gelatin, and 0.25% w/v Irgacure 2959 (we will call it device formulation) solution was mixed in DI water at 50° C and used as hydrogel medium for making the microfluidic channels. For making the devices, this formulation was first cast into an acrylic box by keeping it at 4° C. After that, the formulation solidified due to thermal gelation of both gelatin and GelMA. On top of this solidified layer, 6% w/v laponite in the form of channels was printed. After the laponite was printed, a hot device formulation was poured on top of the printed layer and kept at 4° C. This formed a bilayer of device formulation and it was put under UV light for curing the assembly. Once the top layer was cured, the cured device was taken out of the cast box using a spatula. Now, the device was inverted, and the bottom layer was cured with the UV light. Once both the layers were UV cured, holes were made either from the sides or the top and PBS/water was flushed through the channels. Then, the laponite layer was taken out by pushing the laponite from the holes made at the sides of the device or top of the device. We could print laponite on top of a natural polymer as both had high water content and were hydrophilic and we hypothesized that there would be layer adhesion between laponite and polymer gels. We printed different shapes and sizes of channels.

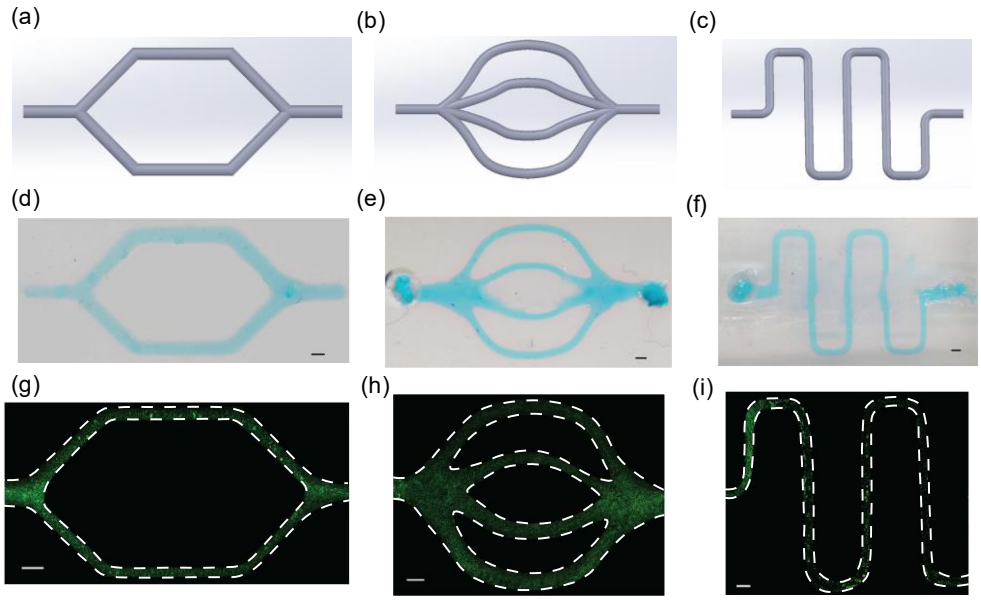

Fig 3.12 Different shapes of microfluidic channels made using nanoclay as sacrificial ink. (a) Bifurcated channels (b) Multibranched and (c) Serpentine channel. Top row (a-c) shows Solidworks design. Middle row (d-f) shows printed channels between two hydrogel layers. Bottom row (g-i) shows perfusion of GFP tagged microbeads through sacrificial channels. (Scale bar: 0.5 mm)

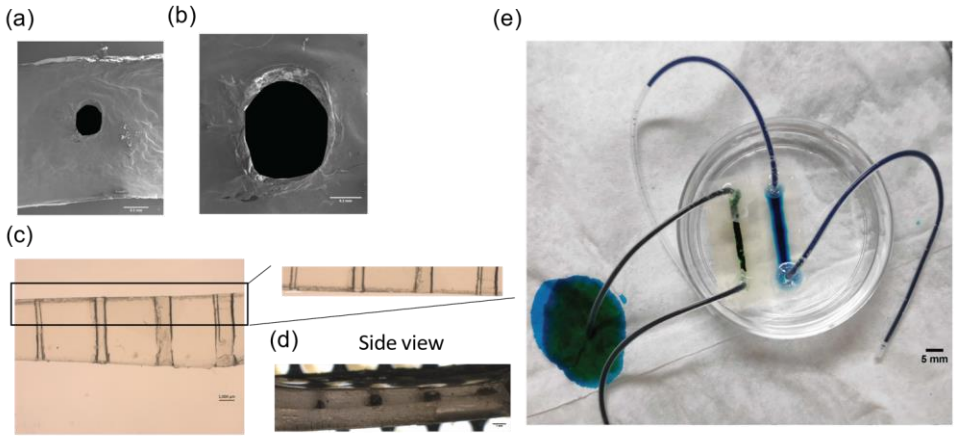

Fig. 3.13 Scanning electron microscopy (SEM) images and versatility of printing. (a) and (b) show SEM micrograph of the shape of the channel (c) shows that different sized channels can be fabricated using Laponite as sacrificial inks (d) show the side view of the different sized channels (e) shows the perfusion of blue and green food dyes inside the channels. (Scale bar: (a) 0.5 mm (b) 0.2 mm (c-d) 1 mm (e) 5 mm)

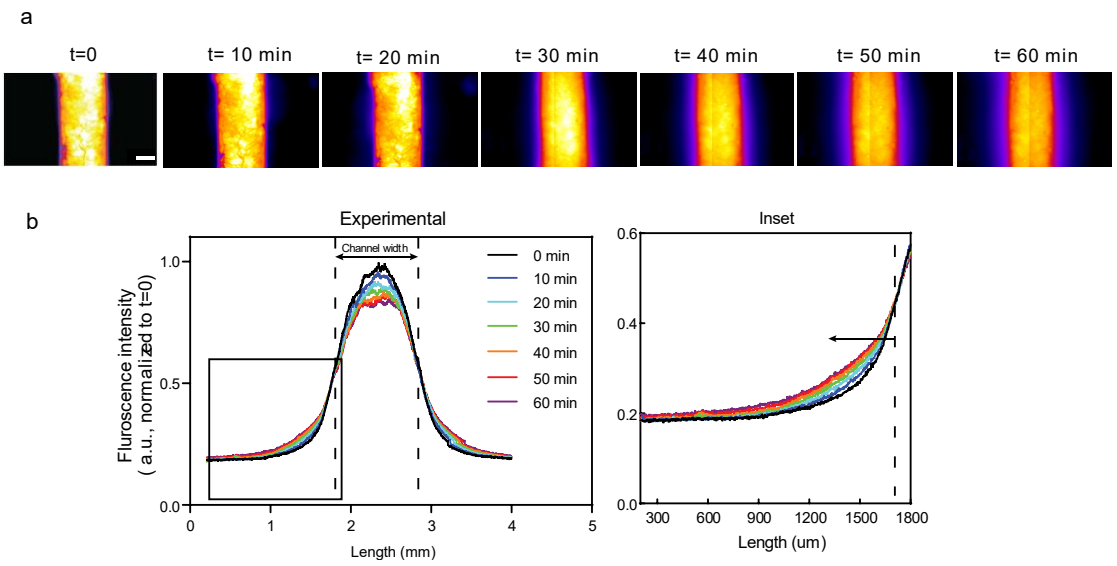

Fig 3.14 Permeability of dextran through a straight channel. (a) Depicts the permeability of 40 KDa FITC tagged Dextran through a straight channel over a time period of an hour. A LUT in ImageJ was used to change the green fluorescent color for better visibility. The fluorescent intensity was plotted (b) to with respect to time and showed a decline inside the channel with time. (Scale bar: 0.5 mm)

3.7.1 Results

We were able to fabricate channels in the hydrogels using Laponite as a sacrificial ink. We fabricated both straight channels and complex channels inside the cast hydrogel formulation. For complex structures, we were able to make bifurcated channels, serpentine channels and multibranched channels (Fig. 3.12). Next, we showed successful FITC labeled microbead perfusion through these channels (Fig. 3.12(g), (h) and (i)). We also printed different sizes of straight channels on the same device to show the versatility of printing. The average size of the channels were about 220 microns, 600 microns, 1000

microns and 1200 microns from thinnest to thickest (Fig. 3.13(c) and (d)). We also showed perfusion of different dyes through the two straight channels in the same device (Fig.3.13(e)). To test the diffusion permeability of the hydrogels, FITC tagged 40kDa dextran was perfused through a 1000 um straight channel and the diffusion was observed for 60 min. This was done to show that various proteins can diffuse through the hydrogel matrix and mass transfer can take place through the channel. The results show the diffusion of dextran with respect to time through the hydrogel material (Fig. 3.14(a)). Diffusion was measured by quantifying the fluorescence intensity inside the channel over 60 min with 10 min time points and the sinusoidal profile (Fig. 3.14(b)) showed the diffusion rate of dextran. This process of making channels inside hydrogel was compared to a previous study[59]. Some of the key differences were they had used a carbohydrate glass mixture (glucose, sucrose, dextran) as the sacrificial material which was warmed at a high temperature of 165° C, extruded at 110° C, vitrified at 50° C to make it hard glass and then a polymer solution was poured around the hard glass. Whereas our study incorporated extrusion of Laponite ink the over the cast polymer at room temperature which is a more facile process. The previous study used polymers to encase the extruded carbohydrate glass around the cast polymer formulation. Our study used a two-step process of layer adhesion of two layers by taking advantage of thermal gelation of polymer formulation. The previous study used a variety of polymers with different crosslinking mechanism whereas we only showed the use of one polymer formulation. The previous study incorporated cells inside their polymers whereas our study didn't incorporate cells in the polymer formulation and cells are supposed to be seeded after the formation of channels.

CHAPTER IV

CONCLUSIONS AND FUTURE WORK

4.1 Conclusions

In conclusion, we were able to achieve the aims and objectives of our research. First, we characterized the different concentrations of Laponite XLG for additive manufacturing applications. This was done using both qualitative and quantitative (rheological) characterization techniques. Then, we were able to 3D print different complex structures of various shapes and sizes using 6% w/v Laponite XLG. Next, we showed that Laponite XLG can be used as a support bath for printing complex structures. This was done by printing different structures such as Texas A&M symbol, pancreas, femur, meniscus, DNA shape, heart, trileaflet valve were printed inside the support bath. Apart from support bath 3D printing, Laponite XLG was also used as a sacrificial ink for making hydrogel based microfluidic devices. We showed that different shape and size channels could be easily printed for making microfluidic devices. We also showed perfusion through these channels. These devices can be used for modelling physiological conditions and diseases. They are better compared to PDMS devices as they allow easy diffusion through the channels which closely mimics actual physiological conditions. Currently, we are investigating the biocompatibility of both the printed constructs inside the support bath and hydrogel based microchannels.

4.2 Future work

In the future, we aim to investigate the biocompatibility of both the channels and printing structures by seeding or encapsulating cells in them:

1. We are investigating the biocompatibility of the printed constructs inside the support bath to see how biocompatible the printed constructs are. This is being done by seeding Human Umbilical Vein Endothelial Cells (HUVECs) on top of the constructs and checking the cell viability.
2. Additionally, for the support bath-based 3D printing, cells need to be incorporated with the extruded material to show its efficacy for 3D bioprinting. For this purpose, different types of cell lines can be used. We will be using (HUVECs) to show the viability. If the support bath is not very biocompatible and cannot support cells, certain compounds or salts would need to be added inside the support bath to make it more biocompatible.
3. We are investigating the biocompatibity of hydrogel microchannel by seeding HUVECs inside them. This will establish that these channels can be used as to mimic vessel like behavior inside the channel. Other types of cells can also be incorporated for modelling the disease behavior inside the channels.

REFERENCES

1. Organ Procurement and Transplantation Network. *Transplant trends*. 2020 [cited 2020 11 February 2020]; Available from: https://unos.org/data/transplant-trends/.

2. Organ Procurement and Transplantation Network. *How we match organs*. 2020 [cited 2020 11 February 2020]; Available from: https://unos.org/transplant/how-we-match-organs/.

3. Langer, R. and J.P. Vacanti, *Tissue engineering.* Science, 1993. **260**(5110): p. 920.

4. Vacanti, J.P. and R. Langer, *Tissue engineering: the design and fabrication of living replacement devices for surgical reconstruction and transplantation.* The Lancet, 1999. **354**: p. S32-S34.

5. U. S. Department of Health and Human Services. *2020: A New Vision - A Future for Regenerative Medicine*. 2005 [cited 2020 14 January, 2020]; Available from: http://singularity-2045.org/HHS-regenerative-medicine-2020-vision-archive-2014.html.

6. Kim, Y.S., et al., *An Overview of the Tissue Engineering Market in the United States from 2011 to 2018.* Tissue Engineering Part A, 2018. **25**(1-2): p. 1-8.

7. Löfgren, H., et al., *Rigid Fusion After Cloward Operation for Cervical Disc Disease Using Autograft, Allograft, or Xenograft: A Randomized Study With Radiostereometric and Clinical Follow-Up Assessment.* Spine, 2000. **25**(15): p. 1908-1916.

8. Mirjam, F., et al., *Tissue Engineered Bone Grafts: Biological Requirements, Tissue Culture and Clinical Relevance.* Current Stem Cell Research & Therapy, 2008. **3**(4): p. 254-264.

9. Wang, W. and K.W.K. Yeung, *Bone grafts and biomaterials substitutes for bone defect repair: A review.* Bioactive Materials, 2017. **2**(4): p. 224-247.

10. Noor, N., et al., *3D Printing of Personalized Thick and Perfusable Cardiac Patches and Hearts.* Advanced Science, 2019. **6**(11): p. 1900344.

11. Pati, F., et al., *Printing three-dimensional tissue analogues with decellularized extracellular matrix bioink.* Nature Communications, 2014. **5**(1): p. 3935.

12. Chen, F.-M. and X. Liu, *Advancing biomaterials of human origin for tissue engineering.* Progress in Polymer Science, 2016. **53**: p. 86-168.

13. Lee, A., et al., *3D bioprinting of collagen to rebuild components of the human heart.* Science, 2019. **365**(6452): p. 482.

14. Grigoryan, B., et al., *Multivascular networks and functional intravascular topologies within biocompatible hydrogels.* Science, 2019. **364**(6439): p. 458.

15. Annabi, N., et al., *25th Anniversary Article: Rational Design and Applications of Hydrogels in Regenerative Medicine.* Advanced Materials, 2014. **26**(1): p. 85-124.

16. Griffith, L.G. and G. Naughton, *Tissue Engineering--Current Challenges and Expanding Opportunities.* Science, 2002. **295**(5557): p. 1009.

17. O'Brien, F.J., *Biomaterials & scaffolds for tissue engineering.* Materials Today, 2011. **14**(3): p. 88-95.

18. Place, E.S., N.D. Evans, and M.M. Stevens, *Complexity in biomaterials for tissue engineering.* Nature Materials, 2009. **8**: p. 457.

19. Discher, D.E., D.J. Mooney, and P.W. Zandstra, *Growth Factors, Matrices, and Forces Combine and Control Stem Cells.* Science, 2009. **324**(5935): p. 1673.

20. Keane, T.J. and S.F. Badylak, *Biomaterials for tissue engineering applications.* Seminars in Pediatric Surgery, 2014. **23**(3): p. 112-118.

21. Drury, J.L. and D.J. Mooney, *Hydrogels for tissue engineering: scaffold design variables and applications.* Biomaterials, 2003. **24**(24): p. 4337-4351.

22. Lee, K.Y. and D.J. Mooney, *Hydrogels for Tissue Engineering.* Chemical Reviews, 2001. **101**(7): p. 1869-1880.

23. Chan, B.P. and K.W. Leong, *Scaffolding in tissue engineering: general approaches and tissue-specific considerations.* European spine journal : official publication of the European Spine Society, the European Spinal Deformity Society, and the European Section of the Cervical Spine Research Society, 2008. **17 Suppl 4**(Suppl 4): p. 467-479.

24. Pina, S., et al., *Scaffolding Strategies for Tissue Engineering and Regenerative Medicine Applications.* Materials (Basel, Switzerland), 2019. **12**(11): p. 1824.

25. Adam, E.J., L.R. Alexandra, and N.S. Ramille, *Advancing the field of 3D biomaterial printing.* Biomedical Materials, 2016. **11**(1): p. 014102.

26. Murphy, S.V. and A. Atala, *3D bioprinting of tissues and organs.* Nature Biotechnology, 2014. **32**: p. 773.

27. Gaharwar, A.K., et al., *2D Nanoclay for Biomedical Applications: Regenerative Medicine, Therapeutic Delivery, and Additive Manufacturing.* Advanced Materials, 2019. **31**(23): p. 1900332.

28. Chimene, D., et al., *Nanoengineered Ionic–Covalent Entanglement (NICE) Bioinks for 3D Bioprinting.* ACS Applied Materials & Interfaces, 2018. **10**(12): p. 9957-9968.

29. Peak, C.W., et al., *Nanoengineered Colloidal Inks for 3D Bioprinting.* Langmuir, 2018. **34**(3): p. 917-925.

30. Wilson, S.A., et al., *Shear-Thinning and Thermo-Reversible Nanoengineered Inks for 3D Bioprinting.* ACS Applied Materials & Interfaces, 2017. **9**(50): p. 43449-43458.

31. Neumann, B.S. and K.G. Sansom, *The rheological properties of dispersions of Laponite, a synthetic hectorite-like clay, in electrolyte solutions.* Clay Minerals, 1971. **9**(2): p. 231-243.

32. Gaharwar, A.K., N.A. Peppas, and A. Khademhosseini, *Nanocomposite hydrogels for biomedical applications.* Biotechnology and Bioengineering, 2014. **111**(3): p. 441-453.

33. Tomás, H., C.S. Alves, and J. Rodrigues, *Laponite®: A key nanoplatform for biomedical applications?* Nanomedicine: Nanotechnology, Biology and Medicine, 2018. **14**(7): p. 2407-2420.

34. Ozbolat, I.T., W. Peng, and V. Ozbolat, *Application areas of 3D bioprinting.* Drug Discovery Today, 2016. **21**(8): p. 1257-1271.

35. Ahu, A.-Y., et al., *Towards artificial tissue models: past, present, and future of 3D bioprinting.* Biofabrication, 2016. **8**(1): p. 014103.

36. Chimene, D., et al., *Advanced Bioinks for 3D Printing: A Materials Science Perspective.* Annals of Biomedical Engineering, 2016. **44**(6): p. 2090-2102.

37. He, Y., et al., *Research on the printability of hydrogels in 3D bioprinting.* Scientific Reports, 2016. **6**: p. 29977.

38. Guvendiren, M., H.D. Lu, and J.A. Burdick, *Shear-thinning hydrogels for biomedical applications.* Soft Matter, 2012. **8**(2): p. 260-272.

39. Carrow, J.K., et al., *Chapter 13 - Polymers for Bioprinting*, in *Essentials of 3D Biofabrication and Translation*, A. Atala and J.J. Yoo, Editors. 2015, Academic Press: Boston. p. 229-248.

40. Duan, B., et al., *Three-dimensional printed trileaflet valve conduits using biological hydrogels and human valve interstitial cells.* Acta Biomaterialia, 2014. **10**(5): p. 1836-1846.

41. Bakarich, S.E., et al., *4D Printing with Mechanically Robust, Thermally Actuating Hydrogels.* Macromolecular Rapid Communications, 2015. **36**(12): p. 1211-1217.

42. Chen, H., et al., *A comparative study of the mechanical properties of hybrid double-network hydrogels in swollen and as-prepared states.* Journal of Materials Chemistry B, 2016. **4**(35): p. 5814-5824.

43. Bhattacharjee, T., et al., *Liquid-like Solids Support Cells in 3D.* ACS Biomaterials Science & Engineering, 2016. **2**(10): p. 1787-1795.

44. Bhattacharjee, T., et al., *Writing in the granular gel medium.* Science Advances, 2015. **1**(8): p. e1500655.

45. O'Bryan, C.S., et al., *Self-assembled micro-organogels for 3D printing silicone structures.* Science Advances, 2017. **3**(5): p. e1602800.

46. O'Bryan, C.S., et al., *Jammed Polyelectrolyte Microgels for 3D Cell Culture Applications: Rheological Behavior with Added Salts.* ACS Applied Bio Materials, 2019. **2**(4): p. 1509-1517.

47. Hinton, T.J., et al., *3D Printing PDMS Elastomer in a Hydrophilic Support Bath via Freeform Reversible Embedding.* ACS Biomaterials Science & Engineering, 2016. **2**(10): p. 1781-1786.

48. Hinton, T.J., et al., *Three-dimensional printing of complex biological structures by freeform reversible embedding of suspended hydrogels.* Science Advances, 2015. **1**(9): p. e1500758.

49. Jin, Y., W. Chai, and Y. Huang, *Printability study of hydrogel solution extrusion in nanoclay yield-stress bath during printing-then-gelation biofabrication.* Materials Science and Engineering: C, 2017. **80**: p. 313-325.

50. Jin, Y., et al., *Granular gel support-enabled extrusion of three-dimensional alginate and cellular structures.* Biofabrication, 2016. **8**(2): p. 025016.

51. Jin, Y., et al., *Functional Nanoclay Suspension for Printing-Then-Solidification of Liquid Materials.* ACS Applied Materials & Interfaces, 2017. **9**(23): p. 20057-20066.

52. Jin, Y., et al., *Printing of Hydrophobic Materials in Fumed Silica Nanoparticle Suspension.* ACS Applied Materials & Interfaces, 2019. **11**(32): p. 29207-29217.

53. O'Bryan, C.S., et al., *Commercially available microgels for 3D bioprinting.* Bioprinting, 2018. **11**: p. e00037.

54. Huang, G.Y., et al., *Microfluidic hydrogels for tissue engineering.* Biofabrication, 2011. **3**(1): p. 012001.

55. Andersson, H. and A.v.d. Berg, *Microfabrication and microfluidics for tissue engineering: state of the art and future opportunities.* Lab on a Chip, 2004. **4**(2): p. 98-103.

56. Gold, K., A.K. Gaharwar, and A. Jain, *Emerging trends in multiscale modeling of vascular pathophysiology: Organ-on-a-chip and 3D printing.* Biomaterials, 2018.

57. Sackmann, E.K., A.L. Fulton, and D.J. Beebe, *The present and future role of microfluidics in biomedical research.* Nature, 2014. **507**: p. 181.

58. Kinstlinger, I.S. and J.S. Miller, *3D-printed fluidic networks as vasculature for engineered tissue.* Lab on a Chip, 2016. **16**(11): p. 2025-2043.

59. Miller, J.S., et al., *Rapid casting of patterned vascular networks for perfusable engineered three-dimensional tissues.* Nature Materials, 2012. **11**: p. 768.

60. Nie, J., et al., *Vessel-on-a-chip with Hydrogel-based Microfluidics.* Small, 2018. **14**(45): p. 1802368.

61. O'Bryan, C.S., et al., *Three-dimensional printing with sacrificial materials for soft matter manufacturing.* MRS Bulletin, 2017. **42**(8): p. 571-577.